

## Diagenesis of Glacimarine Miocene Strata in CRP-1, Antarctica

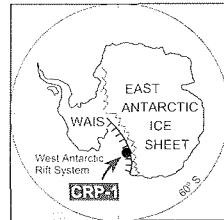
J.C. BAKER<sup>1</sup> & C.R. FIELDING<sup>2</sup>

<sup>1</sup>Centre for Microscopy and Microanalysis, The University of Queensland, Qld, 4072,  
and K.R. Martin Pty Ltd, PO Box 22, Kenmore, Qld, 4069 - Australia

<sup>2</sup>Department of Earth Sciences, The University of Queensland, Qld, 4072 - Australia

Received 14 July 1998; accepted in revised form 18 September 1998

**Abstract** - A diagenetic study was carried out on the cored Miocene section in CRP-1 by thin-section, X-ray diffraction, scanning electron microscope, electron microprobe and stable isotopic analysis. Carbonate (calcite, siderite) microconcretions occur locally within intergranular pores and open fractures, and some sands are cemented by microcrystalline calcite. Calcite cement at 115.12 mbsf (metres below sea floor) and possibly microconcretionary calcite at 44.62 mbsf record infiltration of meteoric waters into the section, consistent with sequence stratigraphic evidence for multiple glacial advances over the CRP-1 drillsite. Diagenetic carbonates incorporated carbon derived from both organic matter and marine carbonate. Carbon isotope data are consistent with microconcretion formation at shallow depths. Sandstones are poorly compacted and, despite containing a large component of chemically unstable grains, are virtually unaltered. Preservation of the chemically unstable grain component reflects the cold climate depositional setting and shallow maximum burial depths.



### INTRODUCTION

CRP-1, Victoria Land Basin, was drilled to a depth of 147.69 mbsf (metres below sea floor) and penetrated a lower Quaternary (Pleistocene) section to 43.15 mbsf (Fielding et al., this volume) unconformably overlying a lower Miocene interval (43.15-147.69 mbsf). This paper presents preliminary results of a petrographic study of the Miocene interval in CRP-1. The prime objective of the study was to identify the principal diagenetic processes and products within the interval with the view of elucidating aspects of its burial, structural and hydrological history. Background stratigraphic information and lithologic logs for CRP-1 are given in Cape Roberts Science Team (1998b, c), and additional information on diagenetic carbonates in the Miocene section is given by Claps & Aghib (this volume).

### METHODS

Thirty-seven samples were taken from mainly sandy lithologies in the working half of the core in Bremerhaven, Germany. Sample points were selected to include fractured lithologies as well as the interval immediately above and below the inferred Quaternary-Miocene unconformity at 43.15 mbsf. Samples were wrapped in aluminium foil at Bremerhaven and transported to Australia as air freight.

All samples were impregnated with blue-dyed epoxy resin and thin-sectioned in kerosene. Many thin-sections were stained for carbonate using Alizarin red-S and potassium ferricyanide. Selected thin-sections from the Miocene section were point-counted (350 points using the Gazzi-Dickinson method) for detrital and diagenetic

mineralogy and visible porosity. Quaternary samples were unconsolidated, clay-rich and generally lacked diagenetic effects, hence were not point-counted for this study, although two Quaternary sands were point-counted in a related study by Fielding et al. (this volume).

X-ray diffraction (XRD) analysis was carried out on the fine fraction of all samples. Samples were analysed in an air-dried state and also following glycolation. Nine samples were examined under a scanning electron microscope (SEM) with an energy dispersive spectrometer (EDS), and four polished thin-sections were analysed with an electron microprobe to provide compositional data on diagenetic carbonates. Backscattered electron imaging was performed during microprobe analysis.

Stable isotopic analysis (carbon and oxygen) was carried out on diagenetic carbonates in six samples. Calcite was reacted for 1 hour at 25°C and siderite for 3 days at 75°C in 100% orthophosphoric acid, to extract carbon dioxide for isotopic analysis (McCrea, 1950). In one sample, separate isotopic analyses were made on coexisting calcite and siderite based on timed extraction of carbon dioxide.

### MINERALOGY AND PETROLOGY

Most samples are fine to medium grained sands and sandstones that lie within the arkose and lithic arkose fields in the classification scheme of Folk et al. (1970) (Fig. 1, Tab. 1). Plagioclase generally dominates over potassium feldspar, and most recorded rock fragments are of volcanic origin. Volcanic rock fragments include crystalline basalt, and mafic and felsic glass. Other igneous rock fragments include dolerite and biotite granite. The heavy mineral assemblage is dominated by pyroxene, and also includes

Tab. 1 - Modal analyses.

Depth (mbsf)	Qtz	Cht	Kfe	Pla	IRF	VRF	MRF	SRF	Glass	Mea	Pyrx	HM	Sid	Cal	Foss	Slp	Opq	Clay	V-P
60.37	40.3	0.3	5.0	9.1	1.4	2.0	0.3	-	8.8	-	4.8	0.3	3.0	5.0	0.6	-	0.6	3.1	15.4
65.76	44.8	-	5.4	12.1	-	0.9	-	-	1.4	-	7.4	0.6	-	-	-	-	-	14.3	13.1
68.57	47.1	0.3	5.0	16.0	-	0.6	-	-	3.0	-	5.1	-	-	-	-	-	0.6	14.3	8.0
89.18	52.3	-	2.6	13.9	0.3	1.4	-	-	0.6	-	5.7	0.3	-	-	-	-	0.3	-	22.6
91.38	39.0	-	1.8	5.5	-	0.8	-	-	-	-	3.5	0.3	-	-	-	0.5	-	0.3	48.3
115.12	32.0	-	8.0	10.3	1.6	4.0	0.3	-	3.0	-	6.4	-	-	34.4	-	-	-	-	-
117.60	40.0	-	4.3	7.7	-	0.6	-	-	1.1	-	8.2	-	-	-	0.3	-	-	1.4	36.4
133.70	42.0	-	4.8	9.6	0.3	0.3	0.3	-	1.0	-	5.4	0.6	8.6	-	-	-	3.8	1.3	22.0
147.46	34.8	-	3.2	8.0	-	0.8	-	-	6.4	-	2.8	0.4	7.2	-	-	-	1.6	28.0	6.8

Note: Qtz = quartz, Cht = chert, Kfe = K-feldspar, Pla = plagioclase, IRF = intrusive igneous rock fragments, VRF = volcanic rock fragments, MRF = metamorphic rock fragments, SRF = sedimentary rock fragments, Glass = volcanic glass, Mea = mica, Pyrx = pyroxene, HM = heavy minerals (excl. pyroxene), Sid = siderite, Cal = diagenetic calcite, Foss = calcareous fossil, Slp = sulphate, Opq = opaques, V-P = visible porosity.

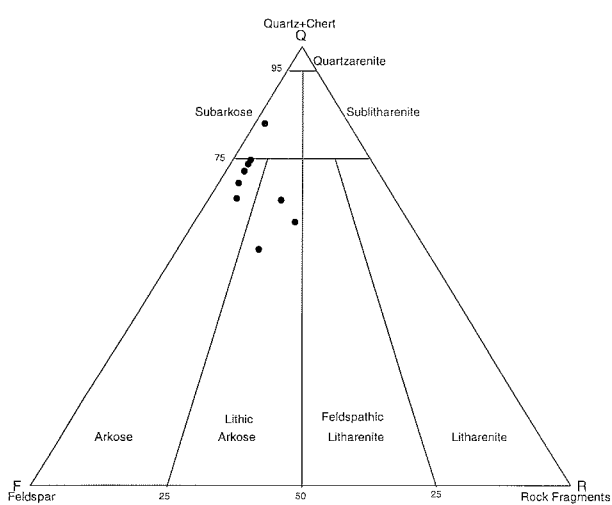


Fig. 1 - QFR compositions of Miocene sandstones.

hornblende, epidote, zircon, olivine, apatite, tourmaline and garnet. Most sands contain abundant visible intergranular porosity as a consequence of being relatively uncompactated.

Diagenetic minerals present are siderite, calcite, pyrite, smectite, and a potassium-calcium-bearing sulphate. Carbonate microconcretions occur in several thin-sections from throughout the cored Miocene interval below 43.60 mbsf, where they partly fill primary intergranular pores and open fractures (Fig. 2a, b). In some samples (*e.g.*, 44.62 and 60.36 mbsf), microconcretions have ferroan calcite interiors and siderite exteriors (Fig. 2c) and have rarely nucleated around biogenic calcite (Fig. 2d), whereas in other samples (*e.g.*, 133.70 and 147.46 mbsf), microconcretions are composed entirely of siderite. All microconcretionary siderite is enriched in magnesium and calcium and depleted in manganese (Fig. 3, Tab. 2). Backscattered electron images clearly illustrate a concentric compositional zonation within some microconcretions (Fig. 2c, d). Carbonate zones are separated by 1-2 µm wide voids (Fig. 2e) that may mark the former location of organic biofilms that controlled microconcretion growth. Compositionally-zoned microconcretions are typically 30-120 µm wide and have a spherical or ovoid shape and irregular surfaces that are made up of fine, subhedral, rhombohedral crystal terminations (Fig. 2f), whereas siderite microconcretions below 125.10 mbsf consist of

relatively small (5-15 µm), single or aggregated spherules and subhedral to euhedral rhombs (Fig. 2g, k). In one sample (74.98 mbsf), authigenic siderite also forms a microcrystalline cement within fine fractures (Fig. 2h).

Microcrystalline calcite cement is abundant in a sample from 115.12 mbsf, where it fills most intergranular pores (Fig. 2i). SEM reveals that the cement consists of loosely packed aggregates of 10-30 µm, elongate bladed crystals (Fig. 2j) that are composed of low-magnesium, ferroan calcite of similar composition to the microconcretionary calcite (Tab. 2). Recognition of patchy calcite cement at intervals through the core was made during re-examination of the archive half in Tallahassee, Florida. Diagenetic calcite was also recorded in thin-sections from between 43.20 and 43.60 mbsf, immediately below the inferred unconformity, where it occurs as finely dispersed, loosely packed, anhedral crystals (10-50 µm) that occupy intergranular areas.

Diagenetic pyrite occurs sporadically within the Miocene section as concretionary cement patches (Fig. 2k) and as isolated octahedra (Fig. 2f). In one sample (91.38 mbsf), a fibrous sulphate mineral that resembles gypsum forms dense mats and isolated rosettes within intergranular pores (Fig. 2l, m). EDS revealed this unidentified mineral is high in sulphur and potassium, and low in calcium. Diagenetic clays are rare, and, if present, are mainly smectite which has formed by alteration of volcanic rock fragments and glass (Fig. 2n). Other clay minerals detected by XRD are minor to trace illite and chlorite, which are of detrital origin.

## DIAGENETIC HISTORY

Sandstones are poorly compacted, rendering any interpretation of diagenetic paragenesis tentative. Furthermore, the limited array and distribution of diagenetic minerals further hampers interpretation of the relative timing of diagenetic events.

### PYRITE

Pyrite, where observed, appears to be the earliest diagenetic mineral. This is because it does not surround carbonate microconcretions, but it does completely surround framework grains, which elsewhere have point grain contacts. Given the marine depositional environment

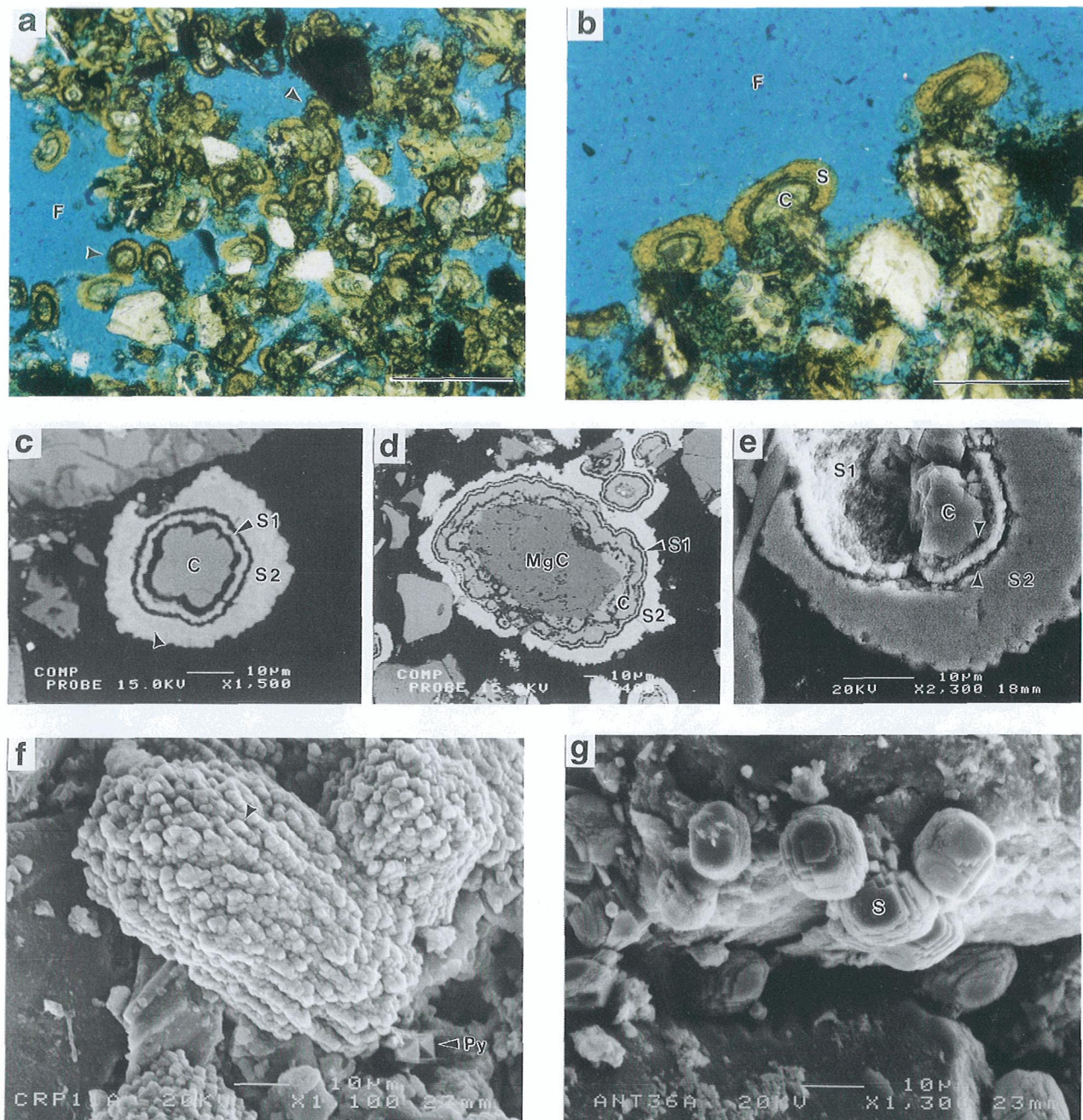


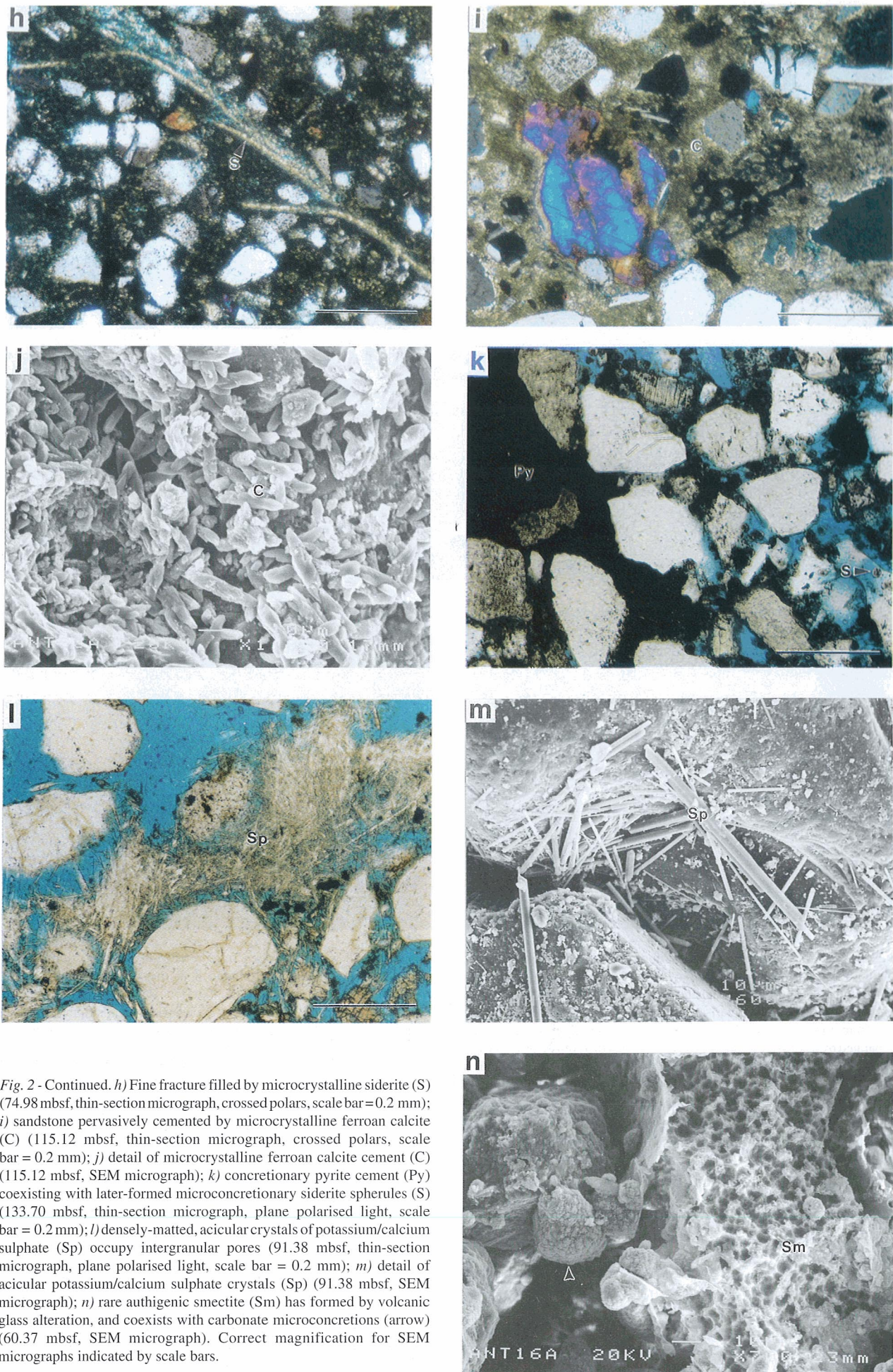
*Fig. 2 – a) Concentrically-zoned carbonate microconcretions (arrows) are concentrated within an open fracture (F) (44.62 mbsf, thin-section photomicrograph, plane polarised light, scale bar = 0.2 mm); b) detail of microconcretions that have precipitated along the side of an open fracture (F). Microconcretions are elongate parallel to fracture and have ferroan calcite (C) interiors and siderite (S) exteriors (44.62 mbsf, thin-section photomicrograph, plane polarised light, scale bar = 0.1 mm); c & d) back scattered electron images highlighting concentric, compositional zonation within microconcretions. Microconcretion in figure 2c has a ferroan calcite interior (C) rimmed by two layers of siderite (S1, S2), each of which is separated by a void (dark rings). A slight contrast difference (arrow) within the S2 layer shows that this layer is compositionally zoned. Microconcretion in figure 2d nucleated around biogenic, high-Mg calcite (MgC), and exhibits the same compositional zonation as microconcretion shown in figure 2c (44.62 mbsf); e) internal structure of a carbonate microconcretion. Part of the ferroan calcite interior (C) was removed during sample preparation to reveal the irregular underside of the inner siderite layer (S1). Calcite interior and siderite inner (S1) and outer (S2) layers are each separated by voids (arrows) that may mark the former location of organic biofilms (44.62 mbsf, SEM micrograph); f) compositionally-zoned microconcretions have irregular surfaces made up of fine, subhedral, rhombohedral siderite crystal terminations (arrow). Very fine pyrite octahedra (Py) are also included in the field of view (44.62 mbsf, SEM micrograph); g) microconcretions consisting of single and aggregated crystals of rhombohedral siderite (S) (133.70 mbsf, SEM micrograph).*

of the host sandstones, pyrite formation is likely to be related to bacterially-mediated sulphate reduction.

#### CARBONATE MICROCONCRETIONS

Carbonate microconcretions are restricted to Miocene strata below 43.60 mbsf. Filling fractures, the micro-

concretions clearly postdate the opening of fractures, the origin of which is unclear. Although there is no evidence to suggest that the fractures formed at or near the surface, the microconcretions could have formed in near-surface environments if significant sediment erosion, subsequent to fracturing, occurred during glacial advances. Sequence stratigraphic evidence suggests that (grounded) glaciers



Tab. 2 - Carbonate microprobe analyses.

Depth (mbsf)	Mineral	Habit	CaCO <sub>3</sub>	MgCO <sub>3</sub>	FeCO <sub>3</sub>	MnCO <sub>3</sub>	SrCO <sub>3</sub>
44.62	calcite	microconcretion #1 interior	95.61	3.23	0.80	0.23	0.13
	siderite	microconcretion #1 middle	11.37	7.16	80.56	0.80	0.11
	siderite	microconcretion #1 exterior	12.60	10.52	76.10	0.73	0.05
	calcite	microconcretion #2 interior	94.64	2.97	1.81	0.45	0.13
	siderite	microconcretion #2 exterior	11.99	7.99	79.11	0.86	0.05
	Mg calcite	microconcretion #3 biogenic calcite nucleus	61.93	37.58	0.23	0.06	0.20
	calcite	microconcretion #3 interior	92.99	1.70	3.53	1.70	0.08
	siderite	microconcretion #3 exterior	12.29	10.05	76.88	0.78	0.00
	calcite	microconcretion #1 interior	92.93	2.03	4.02	0.95	0.07
	siderite	microconcretion #1 exterior	11.22	9.68	78.29	0.78	0.03
60.37	calcite	microconcretion #2 interior	91.23	2.48	4.83	1.38	0.08
	calcite	microconcretion #3 interior	92.66	2.15	3.89	1.15	0.15
	calcite	microcrystalline cement	93.54	2.04	2.74	1.60	0.08
	calcite	microcrystalline cement	89.71	3.28	5.25	1.62	0.14
115.12	calcite	microcrystalline cement	93.20	2.39	2.62	1.66	0.13
	calcite	microcrystalline cement	92.39	2.39	3.59	1.52	0.11
	siderite	microconcretion #1	7.54	19.17	72.27	0.86	0.16
	siderite	microconcretion #2	7.90	19.34	71.78	0.98	0.00
133.70	siderite	microconcretion #3	7.71	18.89	72.64	0.76	0.00
	siderite	microconcretion #4	7.28	20.62	71.22	0.80	0.08

extended beyond the CRP-1 drillsite during periods of glacial advance (Cape Roberts Science Team, 1998a, b).

The oxygen isotopic composition (Tab. 3) of both calcite and siderite in the microconcretions indicates that, if the microconcretions only precipitated from seawater, they would have formed at burial temperatures of 30–45°C (Fig. 4a, b). Alternatively, if the microconcretions formed near the seafloor, where temperatures were unlikely to have exceeded 10°C, their oxygen isotopic composition indicates that pore waters involved in microconcretion formation had  $\delta^{18}\text{O}_{\text{SMOW}}$  values no higher than  $-8.0$  to  $-4.9\text{\textperthousand}$ , which implies that the pore waters included a significant meteoric component. For the siderites, this possibility is downgraded by their consistently high magnesium and calcium and low manganese content (Tab. 2), which is consistent with siderite precipitation from marine pore water (Mozley, 1989). Siderite precipitation was probably microbially mediated, based on textural evidence for the existence of organic biofilms

within the microconcretions (Fig. 2e) and also on the resemblance of siderite below 125.10 mbsf to the microbial siderite shown by Mortimer & Coleman (1997). Accordingly, there is also the possibility that the siderite formed at near-surface temperatures in the presence of unmodified seawater and has anomalously low  $\delta^{18}\text{O}$  values due to the influence of bacteria on the fractionation of oxygen between water and the siderite (Mortimer & Coleman, 1997). Moreover, error may have been introduced by extrapolating the herein used siderite-water fractionation equation of Carothers et al. (1988) to low temperatures ( $<33^{\circ}\text{C}$ ) (see Mortimer & Coleman, 1997). Hence, the siderite oxygen data remain ambiguous. Microbes may have also influenced the oxygen isotopic composition of microconcretionary calcite, but it is worth pointing out that the Miocene section also contains calcite cement that has not been affected by microbes (43.20 and 43.38 mbsf) and that almost certainly has a meteoric isotopic signature (115.12 mbsf) (see below). Accordingly, the possibility that meteoric waters were involved in microconcretionary calcite formation cannot be dismissed.

Microconcretionary calcite at 44.62 mbsf is strongly depleted in  $^{13}\text{C}$  ( $\delta^{13}\text{C}_{\text{PDB}} = -12.5\text{\textperthousand}$ ), indicating that the calcite fixed carbon originating from organic matter rather than marine carbonate. Siderite that encapsulates the calcite is considerably more enriched in  $^{13}\text{C}$  ( $\delta^{13}\text{C}_{\text{PDB}} = -0.1\text{\textperthousand}$ ), and, by contrast, has a carbon isotopic composition consistent with a marine carbonate carbon source. Microconcretionary siderite at 133.70 and 147.46 mbsf is depleted in  $^{13}\text{C}$  ( $\delta^{13}\text{C}_{\text{PDB}} = <-3.6\text{\textperthousand}$ ) compared with siderite

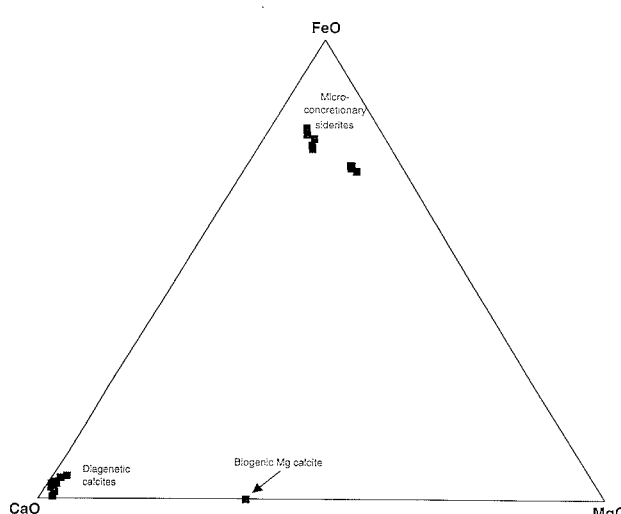


Fig. 3 – Carbonate elemental composition in terms of FeO, CaO and MgO.

Tab. 3 - Carbonate isotope analyses.

Depth (mbsf)	Mineral	Habit	$\delta^{13}\text{C}_{\text{PDB}}$ (%)	$\delta^{18}\text{O}_{\text{SMOW}}$ (%)	$\delta^{18}\text{O}_{\text{PDI}}$ (%)
43.20	calcite	microcrystalline cement	0.1	34.3	3.3
43.38	calcite	microcrystalline cement	0.4	35.0	4.0
44.62	calcite	microconcretion interior	-12.5	26.6	-4.1
44.62	siderite	microconcretion exterior	-0.1	30.7	-0.2
115.12	calcite	microcrystalline cement	-10.2	20.3	-10.2
133.70	siderite	microconcretion	-7.9	27.6	-3.2
147.46	siderite	microconcretion	-3.7	27.5	-3.3

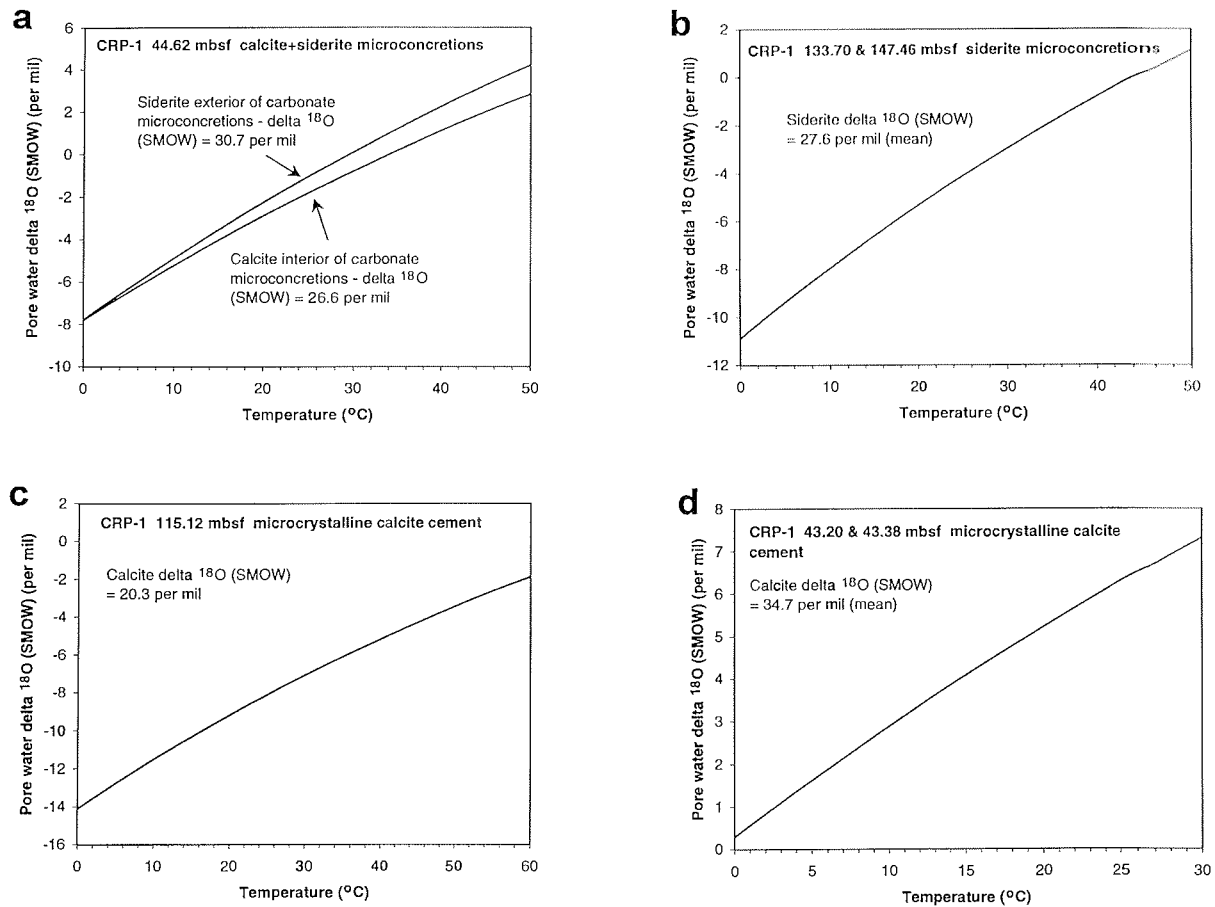


Fig. 4 – Oxygen-isotope fractionation curves for diagenetic carbonates in CRP-1. Curves were calculated using the following mineral-water fractionation equations:

- $1000\ln_{\text{siderite-water}} = 3.13 \times (10^6 T^{-2}) - 3.50$  (Carothers et al., 1988);
  - $1000\ln_{\text{calcite-water}} = 2.78 \times (10^6 T^{-2}) - 2.89$  (Friedman & O'Neil, 1977).
- Note: T = temperature in kelvins.

at 44.62 mbsf, and, from its carbon isotopic composition, appears to have incorporated carbon that was at least partly sourced from organic matter.

The indications are that the cored Miocene section has not been sufficiently buried to allow thermally-mediated decarboxylation reactions (which produce strongly  $^{13}\text{C}$ -depleted bicarbonate) to proceed (see below). Hence, the negative  $\delta^{13}\text{C}$  values of the microconcretionary carbonates point to microconcretion precipitation at shallow (<10 m) burial depths, where strongly  $^{13}\text{C}$ -depleted bicarbonate can be produced in the oxic, sulphate reduction and iron reduction diagenetic zones (Curtis et al., 1986). If fractures that host the microconcretions formed at depth, then evidently sediment was eroded subsequent to fracturing. This process resulted in these fractures being placed within, or being connected to, the very shallow diagenetic zones where  $^{13}\text{C}$ -depleted bicarbonate could be generated.

#### CALCITE CEMENT

The oxygen isotopic composition of calcite cement at 115.12 mbsf indicates that, if this calcite precipitated below 60°C, the pore water must have had a  $\delta^{18}\text{O}_{\text{SMOW}}$  less than  $-1.9\text{\textperthousand}$ , which implies it had a mixed marine-meteoric

origin (Fig. 4c). Nearby non-cemented sands are poorly compacted or unconsolidated, hence it is unlikely that the sediment was sufficiently buried to have reached 60°C (see below). Therefore, it appears that the calcite records infiltration of meteoric waters into the Miocene section, which supports the interpretation that glaciers extended beyond the CRP-1 drillsite during periods of glacial advance (Cape Roberts Science Team, 1998a, b). Like microconcretionary calcite at 44.62 mbsf, calcite cement at 115.12 mbsf is strongly depleted in  $^{13}\text{C}$  ( $\delta^{13}\text{C}_{\text{PDB}} = -10.2\text{\textperthousand}$ ), indicating that the carbon had an organic rather than marine carbonate source. In contrast, calcite cement at 43.20 and 43.38 mbsf has an isotopic composition consistent with precipitation from seawater at just above 0°C (Fig. 4d) and involving carbon derived from marine carbonate.

#### COMPACTION/ALTERATION

Sandstones throughout the cored Miocene section are poorly compacted, with clean sandstones having very high intergranular volumes (up to 48.3%), framework grains having only point-grain contacts, and all ductile grains showing no evidence of having undergone compactional deformation, even in the more compactable

argillaceous lithologies. Clearly, the Miocene section was never deeply buried, as is also suggested by the abundance of unaltered, chemically unstable rock fragments, particularly mafic glassy volcanic rock fragments. If the Miocene section had been deeply buried and thus had been subjected to temperatures well above those at the seafloor, it is expected that many such fragments would have altered. The Miocene sandstones are distinguished by their unusually high content of unaltered, chemically unstable rock fragments and heavy minerals, the preservation of which is probably linked to the cold climate depositional setting as well as to the fact that the sandstones were never deeply buried.

## SUMMARY

Glacimarine Miocene sands and sandstones in CRP-1 locally contain carbonate microconcretions that fill intergranular pores and open fractures. Some microconcretions are concentrically zoned and have a ferroan calcite interior and impure (high Mg and Ca) siderite exterior, whereas other microconcretions consist entirely of impure siderite. Rare fractures are filled by microcrystalline siderite cement, and some sandstones are cemented by pore-filling, microcrystalline, (ferroan) calcite. Other diagenetic minerals include very minor pyrite and a fibrous potassium and calcium-bearing sulphate. Sandstones are poorly compacted and, despite containing abundant chemically-unstable rock fragments and heavy minerals, are remarkably unaltered.

Calcite cement at 115.12 mbsf and possibly microconcretionary calcite at 44.62 mbsf appear to have precipitated from meteoric water, which is consistent with sequence stratigraphic evidence for multiple periods of glacial advance over the CRP-1 drillsite.

Carbon in diagenetic carbonates originated from both organic matter and marine carbonate at shallow (<10m) burial depths. The presence of microconcretions within open fractures may reflect significant sediment-stripping during glacial advances, which resulted in fractured sediments being placed at or very close to the seafloor.

The poorly compacted character of the Miocene section shows that this section was never deeply buried. Preservation of constituent chemically-unstable grains in a virtually unaltered state is linked to the cold climate depositional setting and shallow maximum burial depths.

## ACKNOWLEDGEMENTS

Journal referees W. Dickinson, P. Robinson and M. Claps are thanked for their helpful reviews of the paper. Skilled technical assistance was given by A. Yago and R. Rasch. Isotope analyses were performed in the Stable Isotope Geochemistry Laboratory of the Department of Earth Sciences, The University of Queensland.

## REFERENCES

- Cape Roberts Science Team, 1998a. Miocene Strata in CRP-1, Cape Roberts Project, Antarctica. *Terra Antarctica*, **5**(1), 63-124.
- Cape Roberts Science Team, 1998b. Summary of Results from CRP-1, Cape Roberts Project, Antarctica. *Terra Antarctica*, **5**(1), 125-137.
- Cape Roberts Science Team, 1998c. Appendix 2 - Core Logs. *Terra Antarctica*, **5**(1), 141-175.
- Carothers W.W., Adami L.H. & Rosenbauer R.J., 1988. Experimental oxygen isotope fractionation between siderite-water and phosphoric acid liberated CO<sub>2</sub>-siderite. *Geochimica et Cosmochimica Acta*, **52**, 2445-2450.
- Curtis C.D., Coleman M.L. & Love L.G., 1986. Pore water evolution during sediment burial from isotopic and mineral chemistry of calcite, dolomite and siderite concretions. *Geochimica et Cosmochimica Acta*, **50**, 2321-2334.
- Folk R.L., Andrews P.B. & Lewis D.W., 1970. Detrital sedimentary rock classification and nomenclature for use in New Zealand. *New Zealand Journal of Geology and Geophysics*, **13**, 947-968.
- Friedman I. & O'Neil J.R., 1977. Compilation of stable isotope fractionation factors of geochemical interest. In: Fleischer M. (ed.), *Data of Geochemistry, US Geological Survey Professional Paper*, 6th edition, **440-KK**, 12 p.
- McCrea J.M., 1950. On the isotopic chemistry of carbonates and a palaeotemperature scale. *Journal of Chemical Physics*, **18**, 849-857.
- Mortimer R.J.G. & Coleman M.L., 1997. Microbial influence on the oxygen isotopic composition of diagenetic siderite. *Geochimica et Cosmochimica Acta*, **61**, 1705-1711.
- Mozley P.S., 1989. Relation between depositional environment and the elemental composition of early diagenetic siderite. *Geology*, **17**, 704-706.